Proceedings of the Sixteenth (2006) International Offshore and Polar Engineering Conference
San Francisco, California, USA, May 28-June 2, 2006

ISBN 1-880653-66-4 (Set); ISSN 1098-6189 (Set)

The Wave Field in the Coastal Area of Taipei Harbour

John Z. Yim, Chung-Ren Chou, W-K. Wong & T.-H. Chen
Department of Harbour & River Engineering, National Taiwan Ocean University
Keelung, TAIWAN, China

ABSTRACT

The Taipei Harbour in the northern part of Taiwan is a new harbour presently under construction. A long-time monitoring program of the coastal environments was launched a few years ago. Marine radar is used as the monitoring device.

The Institute of Harbour and River Engineering of the National Taiwan Ocean University started to analyze radar images a few years ago. Wavenumber-frequency spectra were obtained from radar image sequences through 3-D FFT. These were then used to extract information concerning wave heights and wave directions. The results, when compared with records from buoy measurements, were satisfactory. Some preliminary results of our studies are presented in this paper.

KEY WORDS: marine radar, Taipei Harbour, offshore, deep-water, wavenumber-frequency spectra, remote sensing

INTRODUCTION

The industrialization of the world has made nature resources on land closing to the point of exhaustion; flouring world economies have pushed human activities seawards looking for recreation and leisure. All these will have heavy demands on the self-purification ability of the coastal water. On the other hand, sea level rises and increased extreme weather conditions due probably to global warming have raised the threats on coastal erosion. As a result, coastal areas have become more and more important, and this trend will continue in the foreseeable future.

To study wave climate as well as possible environmental impacts of a coastal structure, long-time records are needed. Information concerning wave fields around coastal and/or offshore structures are traditionally collected using wave staffs or buoys. These measuring devices are often denoted as direct measuring devices, since they need to have a direct contact with the water body. Even though these instruments can acquire data directly, but they are limited by the fact that, only point measurements can be performed. To acquire more information of the area under consideration, more devices must be employed. As an alternative, many researchers have applied remote sensing techniques to measure and record the sea surface. Compared with the former devices, the latter have the advantages that information of a relative large area can be acquired instantly.

Extracting information of the sea surface from images has a rather long history. Kinsman (1965) discussed the SWOP (Stereo Wave Observation Project) experiment in some detail. Wavenumber spectra were obtained from stereo photographs. This method was also used by Holthuijsen (1981) to determine directional spectra. Similar works were also carried out by Stilwell & Pilon (1974) and Sugimori (1975).

Detecting the characteristics at the air-sea interface can be roughly divided into two categories. Using radars, one can measure and determine sea state parameters either from a far distance using satellites, or on board of a ship, as well as on land. A rather detailed review of the developments of radar imaging from satellites has been given by Aage et al. (1998) in their monographs. On the other hand, reflections from the rough sea surface, called sea clutter, have long been known to mariners. These reflections are affected by wave height, wind, and antenna height.

Extensive research concerning the usage of marine radar has been carried out by the German research institute GKSS (Senet, 1996; Hatten, 1998; Outzen, 1998; Dankert, 2003), as well as by other researchers around the world (Bell, 1999; Izquierdo et al., 2004, 2005). Compared with satellites, this device has the advantage in that the costs for both acquisition and maintenance are much cheaper than the former.

Simply stated, the operational principals to determine sea state parameters from radar images can be described as follows. Variations of the gray scale intensities are related to the wave height variations. Pixel sizes of digitized images can be treated as spatial discretizations ($\Delta x, \Delta y$) on the *x-y*, i.e., horizontal, plan. A 2D FFT then transforms the gray scale variations to a 2D wavenumber spectrum, where the spectral magnitudes are related to variances of the sea surface. When image sequences are used, as is now the common practice, a 3D FFT is needed and a wavenumber-frequency spectrum can then be obtained.

Even though the principals are rather simple, there are a number of difficulties in practice. For example, there is the so-called 180° ambiguity on the 2D wavenumber spectrum, from which no direction of wave propagation can be correctly determined. There are also noises inherently contained in the images. When the radar is on a moving platform, such as a ship, the velocity of encounter must also be considered. Furthermore, and most importantly, the relation between gray scale intensity and wave height must be empirically determined.

When the radar is at a fixed position, the encounter velocity has no effect (Young et al., 1985; Senet et al., 1997). The 180^o ambiguity of the propagation direction can be resolved, either by determining the phase differences between two consecutive images (Atanassov & Rosenthal, 1985), or through the use of 3D wavenumber-frequency spectra as proposed by Young et al. (1985). Izquierdo et al. (2004, 2005) described comparisons between wave spectra obtained from radar images and those of buoy measurements.

The Taipei Harbour in the northern part of Taiwan is a new harbour presently under construction. A long-time monitoring program of the coastal environments was launched by the Port Authority of Keelung Harbour (PAKH). This program has the purpose of gathering as much information as possible of the coastal processes around the harbour area. The information will then be used to assess possible environmental impacts due to the Harbour; and in the meantime provides fundamental data base for possible further planning in the future. The Institute of Harbour and Marine Technology (IHMT), commissioned for the program, has decided to use marine radar as a monitoring device.

The Harbour and River Engineering of the National Taiwan Ocean University started to study images of wave fields a few years ago (Chou et al., 2004). Wave heights and directions were extracted from wavenumber-frequency spectra obtained from radar image sequences, and compared with results of buoy measurements. In the following, we present some preliminary results of our studies of the wave field of the Taipei Harbour.

THE MEASURING SITE AND INSTRUMENTATION

Taipei Harbour is located at the northern part of the Taiwan, and is approximately 20 kilometers away from Taipei City. The second Danshuei fishing port is on the opposite side of the Harbour. The navigation radar is of type FR-8251 from the Furuno Company, Japan, and is situated atop of the administrative building of the Harbour. From there, it has a view of the whole Danshuei estuary area. In the northern part of Taiwan, the wave field is rather calm in summer seasons, except, when there is a Typhoon nearby. Significant waves of less than 1 meter are quite common in these seasons. On the other hand, relatively strong north to northeast monsoon winds often dominate in winter seasons, and the waves are of the order of 2-3 meters or higher.

The measuring range of the radar is set to 1.5 miles. With a rotation speed of 24 cycles per minute, 32 images, i.e., 80 seconds, per hour of the sea states will be imaged and stored for analysis. A wave observing pile is located outing outside the breakwater. The water depth is 16 meters. A current meter (S4ADW) from the InterOcean Company USA records wave and current conditions on site, and will be used as ground truth for the following analyses. Figure 1 shows the locations of the Harbour (Figure 1, left panel) and instrumentations (right panel) schematically.

The area used for the analysis is marked as a square and shown in Figure 2. It forms an $X = Y = 1011.20 \times 1011.20$ [m] square, approximately. With 128×128 pixels on each side of the image, the interval are $\Delta x = \Delta y = 7.9$ m. As mentioned before, the time interval between each image is $\Delta t = 2.5$ sec, and a total of 80 sec. (32 images) forms an image sequence.

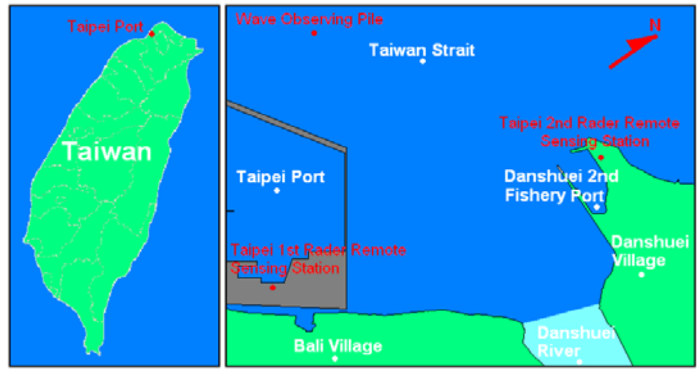

Figure 1 Schematic diagram of the locations of Taipei Port and the instrumentations.

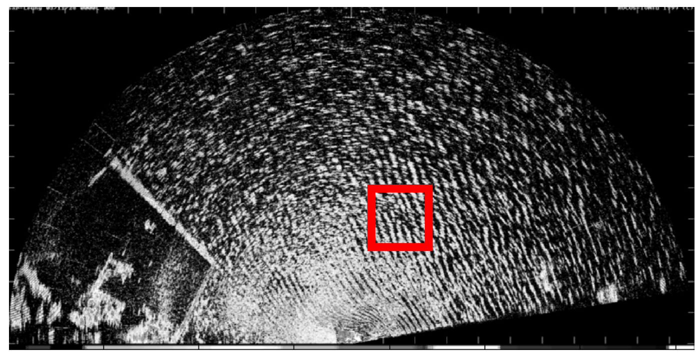

Figure 2 The area used for the analysis.

Gray scales were first extracted from radar images and low-pass filtered to remove high frequency noises (Wong et al., 2004). A three dimensional (3D) FFT is performed with respect to the gray scales of each pixel:

$$G(k_x,k_y,\omega_l) = \left(\Delta k_m \times \Delta k_n \times \Delta\omega_l\right) \sum_{x_m=1}^{M}\sum_{y_n=1}^{N}\sum_{l=1}^{L} g(x_m,y_n,t_l) \times \exp\left[-i2\pi\left(\frac{r_m \Delta k_m}{M} + \frac{r_n \Delta k_n}{N} - \frac{r_l \Delta\omega_l}{L}\right)\right] \quad (1)$$

where

$k_x = r_m \Delta k_m$ (r_m = 1,2,3, …, M) is the wavenumber of the abscissa (2)

$k_y = r_n \Delta k_n$ (r_n = 1,2,3, …,N) is the wavenumber of the ordinate (3)

$\omega_I = r_I \Delta\omega_I$ (r_I = 1,2,3,…, L) is the frequency (4)

$\Delta k_x = \dfrac{2\pi}{M\Delta x}$ is the unit length of the abscissa (5)

$\Delta k_y = \dfrac{2\pi}{N\Delta y}$ is the unit length of the ordinate (6)

$\Delta\omega_I = \dfrac{2\pi}{L\Delta\tau}$ is the unit time of the frequency axis (7)

The wavenumber-frequency spectrum can then be obtained through:

$$S\left(k_x,k_y,\omega_l\right) = \frac{1}{\left(M\Delta x\right)\left(N\Delta y\right)\left(L\Delta\tau\right)}\left|G\left(k_x,k_y,\omega_l\right)\right|^2 \quad (8)$$

where, $X = M\Delta x = Y = N\Delta y = 1011.20$ m is the size of image under consideration, and $T = L\Delta\tau$ = 80 sec. is the duration of the measurement.

RESULTS AND DISCUSSION

Assuming that wave heights are Rayleigh distributed, the significant wave height is then related to the zeroth order of the spectral moment through:

$$H_S = 4\sqrt{m_0} \tag{9}$$

where m_j is the spectral moment is defined as:

$$m_j = \int_0^\infty f^j S(f)\,df = \int_0^\infty f^j \left[\int_{k_y=-\infty}^{\infty} \int_{k_x=-\infty}^{\infty} S(k_x, k_y, f)\, dk_x\, dk_y \right] df \tag{10}$$

Separation of the wave signal from background noise to obtain the so-called signal-to-noise ratio, as was done by many researchers (see, for example, Nieto et al., 1999, Nieto & Guedes Soares, 2000) was not performed at the present. Analyzed are radar images of the sea surface for the time span from November 2003 – September 2004. Figure 3 shows the fits for each month.

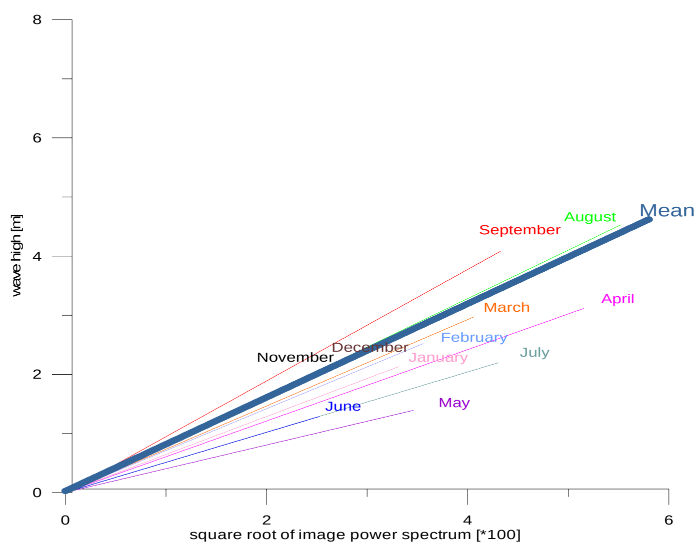

Figure 3 The results of regression analyses for the months Nov. 2003 to Sep. 2004.

It can be seen from Figure 3 that the fits are rather scattered. This is probably due the facts that, a) as mention before, the signal-to-noise ratio has not be determined; b) the data shown in Figure 3 are from all available images, irrespective of the actual weather conditions.

It is well known that, radar images of the sea surfaces are easily affected by the weather. It was pointed out, for example, by many researchers that, rain alters the geometry of the sea surface, as thereby the radar cross section (Craeye et al., 1999; Contreras et al., 2003). Since all the available images were used for the analysis, they certainly must contain those acquired in rainy days. As a result, the goodness of the fit are therefore, degraded. Since, at the moment, there is no easy way to determine whether the images were corrupted by rain, we have decided to choose an alternative way to improve the quality of the fit.

Table 1 lists the standard deviations of the fits. It can be seen from the table that the values do not deviate much from each others. We have therefore decided to use the mean value of the standard deviations of the fit as a criterion to discard/retain the data.

Table 1 Standard deviations of the fits for the months considered

Month Year	Nov. 2003	Dec. 2003	Jan. 2004	Feb. 2004	Mar. 2004	Apr. 2004
Stand. Dev.	0.47	0.52	0.54	0.43	0.48	0.57
Month Year	May 2004	June 2004	Jul. 2004	Aug 2004	Sep. 2004	Mean
Stand. Dev.	0.50	0.38	0.41	0.67	0.64	0.51

It is well known that, when the errors of the measurements are randomly distributed, they seldom exceed 2 times the standard deviation from the mean value, i.e., $x \le \bar{x} \pm 2\sigma_x$, where x is the data point. Assuming that the deviations caused by weather conditions are also randomly distributed, we then exclude about 3.07% of the total data. The result is shown in Figure 4.

Figure 4 shows the result of the new fit (purple, dashed line) together with the original fit (red, straight line). It can be seen that the new result is more satisfactory. This can also be seen from Figure 5, where comparisons with wave heights from the ground truth are shown for each month.

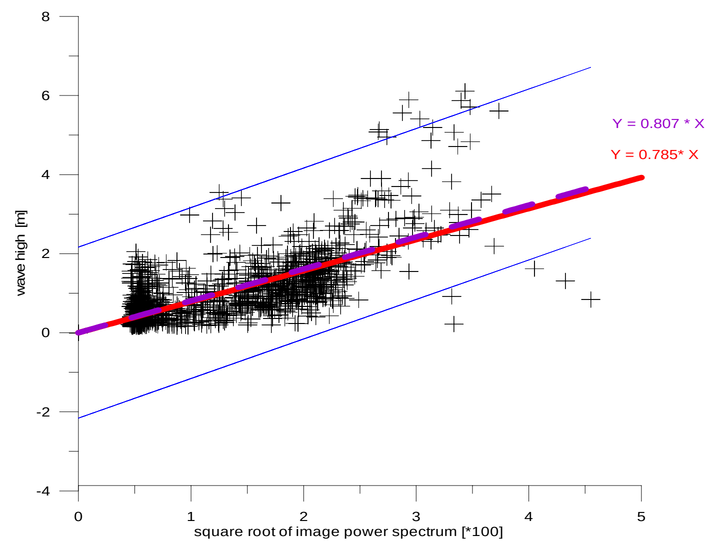

Figure 4 Comparison of the new fit (purple line) with the original (red line)

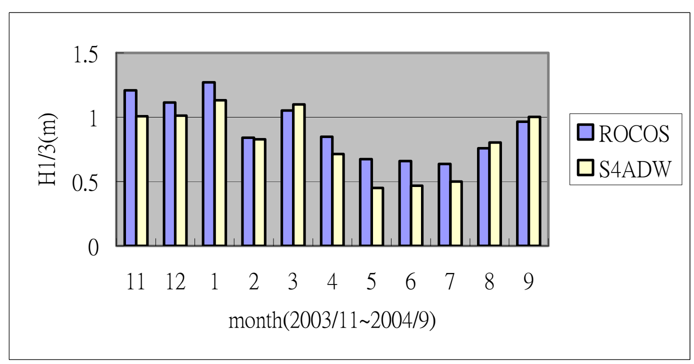

Figure 5 Comparisons with wave heights from ground truth for each

month.

Shown in Figure 5 are the mean values of wave heights estimated from both devices. It can be seen from Fig. 5 that, the differences between the wave heights due to these two instrumentations are relatively high in the months May, June, and July. As mentioned earlier, the waves are relatively low, and the sea surface can be called flat in these months. Quite often, the radar images are blurred by the background noises. It is conjectured that this might affect the estimates. Similar results can also be seen in Figure 5 of Izquierdo et al. (2005), where low wave heights are often overestimated.

Figures 6~8 show the directions of wave propagation estimated from radar images, together with those obtained from S4ADW. The direction of propagation can be found by comparing two consecutive 2D wavenumber spectra from radar images. Atanassov & Rosenthal (1985) have demonstrated that, in this way, the 180° ambiguity can be removed. Three months of results are shown. These are, November 2003, January and June 2004. It can be seen from these figures that, as compared with those from S4ADW, the main direction of wave propagations are estimated correctly. In all these figures, however, there are cases where waves are coming from WNW as estimated from radar images. The reason for this deviation is not clear at present. More studies are needed.

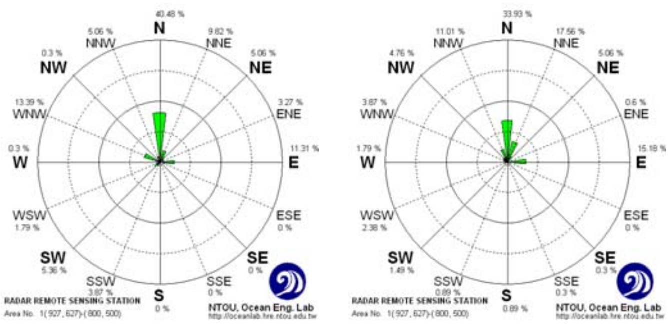

Radar image (2003/11) rose diagram   S4ADW (2003/11) rose diagram

Figure 6. Comparison between radar image rose diagram and S4ADW rose diagram (2003/11).

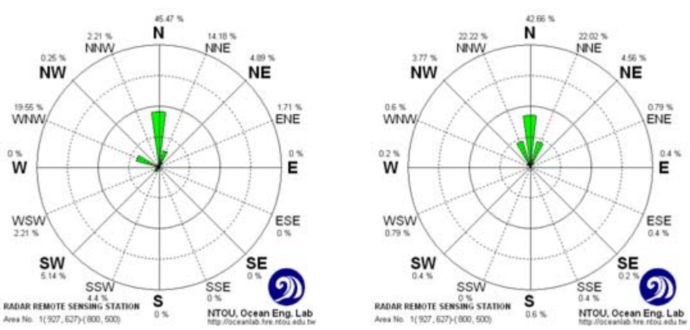

Radar image (2004/1) rose diagram   S4ADW (2004/1) rose diagram

Figure 7. Comparison between radar image rose diagram and S4ADW rose diagram (2004/1).

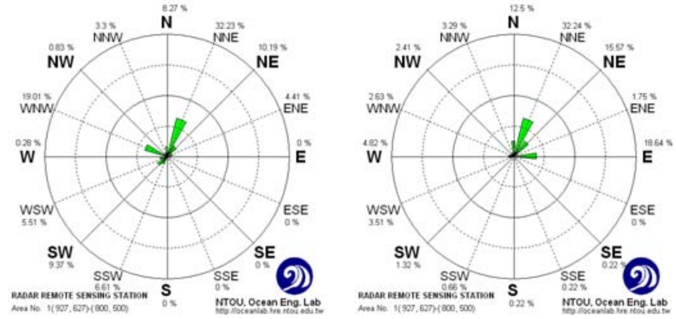

Radar image (2004/6) rose diagram   S4ADW (2004/6) rose diagram

Figure 8. Comparison between radar image rose diagram and S4ADW rose diagram (2004/6).

CONCLUSIONS

Radar images taken in the coastal area of Taipei Harbour were analyzed and some of our preliminary results are shown in this paper. It is shown that both our estimated wave heights and wave directions are comparable with the ground truth. The averaged deviations from ground truth are in the range of ± 12% for wave heights, which are believed to be acceptable. However, it must be admitted that, there are still have a lot of unresolved problems. One of the main difficulties is that transferring from radar images into gray scales is rather time-consuming at present. This hinders the use of estimated results as an on-line system which we are presently working on.

REFERENCES

Aage, C, Allan TD, Carter DJT, Lindgren G, and Olagnon M (1998). “Oceans from space – A textbook for offshore engineers and naval architects” Ifremer, Brest, France, 168 pp.

Atanassov, V, and Rosenthal, W (1985). “Removal of ambiguity of two-dimensional power spectra obtained by processing ship radar images of ocean waves” *J. Geophys. Res.*, Vol. 90, C1, pp. 1061-1067.

Bell, PS (1999). “Shallow water bathymetry derived from an analysis of X-band marine radar images of waves” *Coastal Engineering*, Vol. 37, pp. 513-527.

Chou, CR, Yim JZ, and Huang WP (2004). “Determining the hydrographic parameters of the water surface from image sequences of CCD camera” *Experiments in Fluids*, Vol. 36, pp. 515-527.

Contreras, RF, Plant, WJ, Keller, WC, Hayes, K, and Nystuen, J (2003). “Effects of rain on Ku-band backscatter from the ocean” *Journal of Geophysical Research*, Vol. 108, No. C5, 3165, doi:10.1029/2001JC001255.

Craeye, C, Sobieski, PW, and Bliven, LF (1999). “Radar signature of the sea surface perturbed by rain” *Proceedings of the IEEE 1999 International Geoscience and Remote Sensing Symposium*, IGARSS '99, 28 June-2 July 1999, Vol. 1, pp. 206-208.

Dankert, H (2003). “Measurement of waves, wave groups and wind fields using nautical radar-image sequences” PhD Dissertation, University of Hamburg, 105 pp.

Hatten, H (1998). “On the correlation of the spectral noise of a nautical radar on the wind velocity vector” Master thesis, University of Hamburg, GKSS report number: 98/E/62, 86 pp. (in German)

Holthuijsen, LH (1981). “The directional energy distribution of wind v generated waves as inferred from stereophotographic observations of the sea surface” PhD dissertation, Technical University Delft, 193 pp.

Izquierdo, P, Guedes Soares, C, Nieto Borge, JC, and Rodríguez, GR (2004). “A comparison of sea-state parameters from nautical radar images and buoy data" *Ocean Engineering,* Vol. 31, pp. 2209-2225.

Izquierdo, P, Nieto Borge, JC, Guedes Soares, C, Sanz González, R, and Rodríguez, GR (2005). "Comparison of wave spectra from nautical radar images and scalar buoy data" *Journal of Waterway, Port, Coastal, and Ocean Engineering,* ASCE, Vol. 131 (3), pp. 123-131.

Kinsman, B (1965). "Wind waves, their generation and propagation on the ocean surface" Prentice-Hall, Inc., Englewood Cliffs, New Jersey, 676 pp.

Nieto, JC, Reichert, K, and Dittmer, J (1999). "Use of nautical radar as a wave monitoring instrument" *Coastal Engineering*, Vol. 37, pp. 331-342.

Nieto, JC, and Guedes, C (2000). "Analysis of directional wave fields using X-band navigation radar" *Coastal Engineering*, Vol. 40, pp. 375-391.

Outzen, O (1998). "Bestimmung der Wassertiefe und der oberflächennahen Strömung mit einem nautischen Radar" Master thesis, University of Hamburg, 91 pp. (in German)

Senet, CM (1996). "Untersuchung zur Bestimmung der oberflächennahen Strömungsgeschwindigkeit mit einem nautischen Radar" Master thesis, University of Hamburg, 121 pp. (in German).

Senet, CM, Seemann, J, and Ziemer, F (1997). "An Iterative Technique to Determine the Near Surface Current Velocity from Time Series of Sea Surface Images", *Proc. Oceans "97 MTS/IEEE Conference*, 500 Years of Ocean Exploration, 6-9 Oct. 1997, Halifax, Nova Scotia, Canada, Vol. 1, pp. 66-72.

Stilwell, DJr, and Pilon, RO (1974). "Directional spectra of surface waves from photographs" *Journal of Geophysical Research,* Vol. 79, No. 9, pp. 1277-1284.

Sugimori, Y (1975). "A study of the application of the holographic method to the determination of the directional spectrum of the ocean waves" *Deep-Sea Research,* Vol. 22, pp. 339-350.

Young, IR, Rosenthal, W, and Ziemer, F (1985). "A three-dimensional analysis of marine radar images for the determination of ocean wave directionality and surface currents" *Journal of Geophysical Research,* Vol. 90, No. C1, pp. 1049-1059.

Wong, WK, Lin, TW, and Chou, CR (2004). "Wave Direction Determined by Ra C. R.dar Image Sequences " *Proceedings of the 26th Ocean Engineering Conference in Chinese,* pp .191-197.